Toxicology 363–364 (2016) 19–28

Contents lists available at ScienceDirect

Toxicology

journal homepage: www.elsevier.com/locate/toxicol

# On the contribution of the phagocytosis and the solubilization to the iron oxide nanoparticles retention in and elimination from lungs under long-term inhalation exposure

M.P. Sutunkova[a], B.A. Katsnelson[a,*], L.I. Privalova[a], V.B. Gurvich[a], L.K. Konysheva[a], V.Ya. Shur[b], E.V. Shishkina[b], I.A. Minigalieva[a], S.N Solovjeva[a], S.V. Grebenkina[a], I.V. Zubarev[b]

[a] The Ekaterinburg Medical Research Center for Prophylaxis and Health Protection in Industrial Workers of the Rospotrebnadzor, Ekaterinburg, Russia
[b] The Ural Center for Shared Use "Modern Nanotechnology", Ural Federal University, Ekaterinburg, Russia

ARTICLE INFO

*Article history:*
Received 20 May 2016
Received in revised form 6 July 2016
Accepted 12 July 2016
Available online 14 July 2016

*Keywords:*
Iron oxide
Nanoparticles
Pulmonary toxicokinetics
System modeling

ABSTRACT

The aim of our study was to test a hypothesis according to which the pulmonary clearance *vs.* retention of metal oxide nanoparticles (NPs) is controlled not only by physiological mechanisms but also by their solubilization which in some cases may even prevail.

Airborne $Fe_2O_3$ NPs with the mean diameter of $14 \pm 4$ nm produced by sparking from 99.99% pure iron rods were fed into a nose-only exposure tower. Rats were exposed to these NPs for 4 h a day, 5 days a week during 3, 6 or 10 months at the mean concentration of $1.14 \pm 0.01$ mg/m$^3$. NPs collected from the air exhausted from the exposure tower proved insoluble in water but dissolved markedly in the cell free broncho-alveolar lavage fluid supernatant and in the sterile bovine blood serum. The $Fe_2O_3$ content of the lungs and lung-associated lymph nodes was measured by the Electron Paramagnetic Resonance (EPR) spectroscopy.

We found a relatively low but significant pulmonary accumulation of $Fe_2O_3$, gradually increasing with time. Besides, we obtained TEM-images of nanoparticles within alveolocytes and the myelin sheaths of brain fibers associated with ultrastructural damage.

We have developed a multicompartmental system model describing the toxicokinetics of inhaled nanoparticles after their deposition in the lower airways as a process controlled by their (a) high ability to penetrate through the alveolar membrane; (b) active endocytosis; (c) *in vivo* dissolution.

To conclude, both experimental data and the identification of the system model confirmed our initial hypothesis and demonstrated that, as concerns iron oxide NPs of the dimensions used, the dissolution-depending mechanisms proved to be dominant.



## 1. Introduction

One of the physico-chemical properties of metal and, in particular, metal-oxide nano-particles (Me-NPs) is that, being virtually insoluble in de-ionized water, they do (depending on chemical composition) get more or less solubilized *in vitro* in biological milieus. This suggests that Me-NPs are most likely to be similarly solubilized *in vivo*.

The toxicological importance of such dissolution is not only to be expected *a priori* (Utembe et al., 2015) but is also supported by experimental findings, including our own data obtained under subchronic intra-peritoneal exposure of rats repeatedly to metallic silver NPs in comparison with much less soluble NPs of metallic gold (Katsnelson et al., 2013), and especially to nanoparticles of copper oxide (Privalova et al., 2014) and manganese oxide (Minigalieva et al., 2015). At the same time, the predominant accumulation of NPs in the RES-cell rich organs (liver and spleen) which has been well-established in numerous experiments including our own studies involving the above-mentioned and other Me-NPs (Katsnelson et al., 2010, 2015), suggests the essential toxicokinetic role of NP phagocytosis by resident macrophages.

Of special interest is, however, the comparison of the impacts produced by solubility and phagocytosis on the fate of NPs deposited onto the free surface of the so called 'pulmonary region'

* Corresponding author.
*E-mail address:* bkaznelson@etel.ru (B.A. Katsnelson).

http://dx.doi.org/10.1016/j.tox.2016.07.006
0300-483X/

of the lungs under long-term inhalation exposure. This type of exposure is particularly important for just the metal-oxide NPs because, along with so-called engineered NPs widely manufactured for different technical, scientific and medical usages, there exists a lot of respective nanoscale by-products, namely a substantial fraction of nanoscale ("ultrafine") particles of the above-mentioned chemical composition within the particle size distribution of condensation aerosols generated by arc-welding and various metallurgical technologies and thus polluting the workplace air and ambient air of respective industries. Specifically, $Fe_2O_3$-NPs, along with other chemical species of iron and other metals as well as with micro-scale particles of the same iron oxide, constitute a higher or lower proportion of this pollution depending on different technological parameters (International Institute of Welding, 2009; Lehnert et al., 2012; Ennan et al., 2013; Lewinski et al., 2013).

The aerodynamic mechanisms defining the primary deposition of inhaled NPs predominantly in the pulmonary region of the lungs and in the nasal passages have been long established in science and included into the well-known Lung Deposition Model of the International Commission on Radiological Protection (ICRP, 1994). Subsequently updated quantitative estimates of this deposition based on various mathematical models cannot be regarded as fundamentally different (e.g. Kolanjiyil, 2013; Kreyling et al., 2013). In the meantime, differences of opinion concerning the role of the physiological and physico-chemical mechanisms controlling the further destiny of deposited NPs should just be characterized as fundamental. Up to the present time, there are not enough specific experimental and modelling estimates of the Me-NP dissolution's contribution for any generalizations to be made, and even if this role was experimentally estimated as low in relation to $TiO_2$-NPs (Creutzenberg, 2013), it is most likely to be a special case rather than a general pattern. For example, Adamcakova-Dodd et al. (2014) exposed mice sub-acutely and sub-chronically to ZnO-NPs in an inhalation experiment and found a transient initial phase of substantial increase in the concentration of $Zn^{2+}$ ions in the BALF, which indirectly points to the dissolution of these NPs even before their penetration into the pulmonary interstice. Dumkova et al. (2016) who subjected mice to the round-the-clock inhalation exposure to 12 nm CdO-NPs during 6 weeks registered the accumulation of persistent NPs not only in lungs but in different other organs but did not discussed a possible toxicokineric role of their dissolution.

Kolanjiyil (2013) developed and described in detail in his thesis a very interesting multicompartmental system model for the kinetics of deposition and retention of inhaled NPs in the lungs the parameters of which he estimated based on several published experimental studies involving various Me-NPs under short-term inhalation exposures, in low concentrations as a rule. In this model he assumed the insolubility of these NPs as one of the basic premises. On the contrary, Katsnelson et al. (2010) suggested that the multicompartmental system model of Me-NPs toxicokinetics they proposed should include additional hypothetical flows of solubilized NPs eliminated from the lungs and lung-associated lymph nodes into the blood and lymph, emphasizing however that they did not yet have any data for quantitative identification of these flows.

As for modeling the role of pulmonary phagocytosis, the author of the above-mentioned thesis noted that "Katsnelson et al., 1992 published a multi-compartmental retention model of bio persistent particles in the pulmonary region of the lung. They included [*into the model*] neutrophils which also are engaged in phagocytosis and contribute to alveolar clearance by transfer with their particle load onto the mucociliary escalator". Nevertheless, the model suggested by Kolanjiyil (2013) himself does not allow for this mechanism and presents the alveolar macrophage (AM), in full correspondence with the prevailing tradition, as not the main but the only phagocytal effecter of the nanoparticle pulmonary clearance. This rather essential issue will be considered in more detail in the Discussion Section.

It should be also noted that it is not only for Me-NPs but for micrometric mineral dust particles as well that the role of differences in the low solubility is not always negligibly small not to exert any influence on the pulmonary toxicokinetics. Thus, there is evidence of faster clearance of rat lungs from silicon dioxide (accompanied with involution of silicotic nodules) a few months after discontinuing a long-term exposure of rats to an industrial condensation aerosol of this material compared with a similar exposure to the same concentration of quartz dust (Petin, 1978). Also, silicon dioxide was observed to accumulate at a slower rate in the pulmonary tissue as a result of inhalation exposure to particles of fused silica and, particularly, of dry colloidal silicic acid in comparison with crystalline silica despite equal mass concentrations and similar particle size distributions of respective aerosols in the inhalation chambers (Podgayko et al., 1982; Katsnelson et al., 1984a,b). Moreover, the same structural and surface features of those amorphous silica particles that render them *more soluble* as compared with quartz have also been observed to determine their *higher cytotoxicity* for macrophages, which should have caused *less* efficient elimination but did not. In other words, in these comparative experiments, the role of dissolution in the process of particle elimination proved to be rather noticeable. All this has a direct bearing on the analysis of Me-NP pulmonary toxicokinetics considering the fact that their *in vivo* solubilization and toxicity vary (both uni- and contradirectionally) in a rather wide range.

Starting from the above theoretical premises and previously gathered research experience, we chose for the present study an aerosol of iron oxide ($Fe_2O_3$) particles in the lower nanoscale range. The choice was made partly because we expected these NPs to be of a non-negligible *in vivo* solubility while not featuring too high a toxicity. Another reason for this choice was practical: as stated above, $Fe_2O_3$ particles (nanoscale included) constitute a major proportion of welding fumes and steel metallurgy emissions, and thus many thousands of workers all over the world are exposed to their inhalation impact (Lewinski et al., 2013).

Thus, the aim of this study was to test (taking the pulmonary toxicokinetics of iron oxide NPs as a case study) the consistency of a working hypothesis according to which the pulmonary clearance *vs.* retention of metal oxide nanoparticles (NPs) is controlled not only by phagocytosis-dependent physiological mechanisms but also by the NP solubilization which in some cases may even prevail.

## 2. Materials and methods

### 2.1. Experimental techniques

Airborne iron oxide NPs were obtained by sparking from 99.99% pure iron rods using the Palas DNP-3000 generator and fed into a nose-only exposure chamber/tower (CH Technologies, USA) for 60 rats. An analogous chamber was used for a sham exposure of control rats.

As can be shown by the SEM imaging (Fig. 1) NPs collected on the polycarbonate filter have spherical form and either are singlet or form small aggregates. The latter, when being rather compact were measured as one particle, and even with such approach, the particle size distribution (Fig. 2) proved rather clean-cut and restricted to the nanometric range with mean (±s.d.) diameter $14 \pm 4$ nm.

The chemical identity of the NPs sampled on the filters was confirmed by the Raman spectroscopy to be $Fe_2O_3$ (Fig. 3).

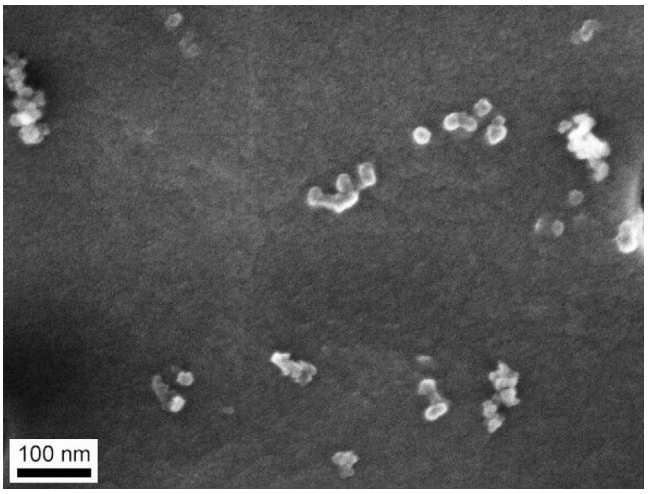


**Fig. 1.** Scanning electron microscopy (SEM) images of nanoparticles accumulated on a polycarbonate filter from the exposed rats breathing zone.

We studied the dissolution of $Fe_2O_3$-NPs accumulated on the microporous PSI filter (Performance Systematix, Inc.—USA) from the air exhausted from the exposure chamber in water, in the normal saline, in the cell-free BALF supernatant or in the sterile bovine blood serum. The $Fe^{2+}$ content was measured on frozen filters by the Electron Paramagnetic Resonance Spectroscopy (EPR) method using the Bruker EMXplus EPR Spectrometer (USA) with an operating microwave frequency of 9–10 Hz at a temperature of ~177 Ê. The first-order derivative of the absorption spectrum was recorded. The integrated intensity (the area under the absorption signal) which is proportional to the mass of the iron in the sample was determined by double integration. For revealing the reduction of the mass of the iron on the filter depending on exposure time in the fluid, the filter was extracted in preset intervals (from 30 min to 8 days on a log scale) for performing EPR measurement and then was again placed in the vessel with the fluid being studied.

The animal experiment was carried out on outbred white female rats from our own breeding colony with initial age about 3 months and initial body mass 193.8 ± 1.8 g in the NP-exposed group and 193.9 ± 1.2 g in the sham-exposed one. All rats were housed in conventional conditions (dry bulb temperature 20–22 °C, relative humidity 50–60%), breathed unfiltered air and were fed standard balanced food and clean bottled water. The study was planned and implemented in accordance with the "International guiding principles for biomedical research involving animals" developed by the Council for International Organizations of Medical Sciences and approved by the Commission for the Bio-Ethics of our Research Center.

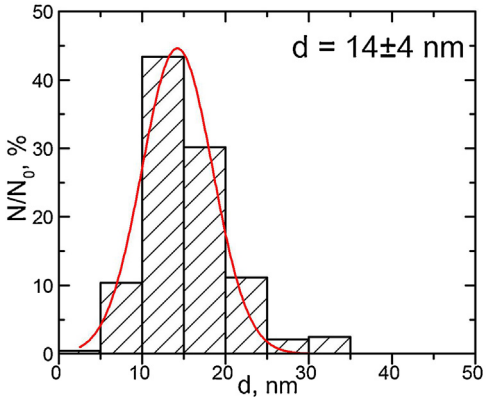


**Fig. 2.** Particle or their aggregate size distribution function obtained by statistical processing of 250 ($N_0$) measured SEM NPs images.

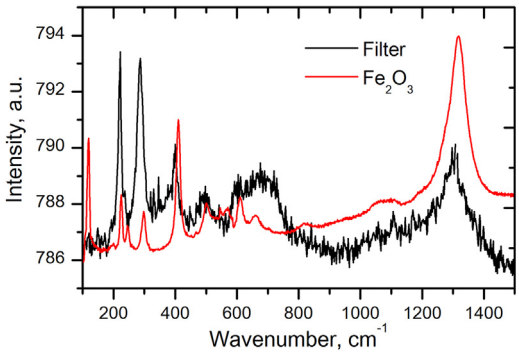


**Fig. 3.** Raman scattering spectrums of the substance collected on filters (black) and of the etalon $Fe_2O_3$ (red). (For interpretation of the references to colour in this figure legend, the reader is referred to the web version of this article.)

After a 2 weeks training necessary to accustom rats to lie still in a correct position within the restraining tubes for the nose-only inhalation NP or the sham exposure, they were so exposed for 4 h a day, 5 days a week over periods of 3, 6 or 10 months and then sacrificed by quick decapitation.

The mean (±s.e.) concentrations of NPs (being fairly uniform in all tiers of the exposure "tower") for these periods were 1.00 ± 0.12, 1.09 ± 0.10 and 1.14 ± 0.02 mg/m$^3$, respectively. Earlier Katsnelson et al. (2010, 2011) proved that 10 nm and even 50 nm iron oxide ($Fe_3O_4$) particles are far more toxic as compared with respective 1 μm particles. Assuming that $Fe_3O_4$ and $Fe_2O_3$ are of similar toxicity and taking in considerations that safe workplace air levels established for $Fe_2O_3$ dusts in different countries vary between 5 and 10 mg/m$^3$, Katsnelson et al. (2012). proposed a reference level for engineered iron oxide NPs in workroom air equal to 0.4 mg/m$^3$ (as TWA), Thus we may tentatively assess the levels actually attained in this inhalation chamber (which are about 2.5 times higher but acting for a 2 times shorter "workshift") as lying close enough to the range of human exposure levels of practical significance.

The $Fe_2O_3$ content of the lungs was measured by the Electron Paramagnetic Resonance Spectroscopy (EPR) method with the Bruker EMXplus EPR Spectrometer (USA). Besides, after 6 and 10 month exposure the pulmonary and brain accumulation of the NPs was visualized with the transmission electron microscopy (TEM). To this end, the pieces of an organ were fixed in 2% paraformaldehyde and 2.5% glutaraldehyde in a cacodylate buffer with 5% sucrose at pH 7.3, then post-fixed in 1% osmium tetroxide, contrasted with uranyl acetate en bloc and embedded in epoxy resin (Spurr). This sample preparation procedure was carried out in a microwave tissue processor, HISTOS REM (Milestone, Italy). Semi-thin (900 nm thick) sections of epoxy blocks were stained in toluidine blue with the addition of 1% borax and examined under the optical microscope for choosing a site for TEM. The 60 nm ultrathin sections of this site obtained with the help a ultramicrotome (Power Tome, «RMC», the USA) were contrasted with uranyl acetate and lead citrate. Grid-mounted sections were investigated in an electron microscope, AURIGA («Carl Zeiss; MT», Germany) in the STEM mode in the range of magnifications 1200–200000.

Total and differential cell counts of the BALF were assessed 24 h after (a) the cessation of each inhalation exposure period and (b) a single intratracheal instillation of the $Fe_2O_3$-NPs obtained by laser ablation of the same pure iron in de-ionized water or of standard quartz dust DQ12 with particle size of less than 5 mcm. To this end, a cannula connected to a Luer's syringe containing 10 mL of normal saline was inserted into the surgically prepared trachea of a rat

under hexenal anesthesia. The fluid entered the lungs slowly under the gravity of the piston, with the animal and syringe positioned vertically. Then the rat and the syringe were turned 180°, and the bronchoalveolar lavage fluid (BALF) flowed back into the syringe. The extracted lavage fluid was poured into siliconized refrigerated tubes. An aliquot sample of the lavage fluid was drawn into a WBC count pipette together with 3% acetic acid and methylene blue. Cell count was performed in a standard hemocytometer (the so-called Goryayev's Chamber). For cytological examination, the BALF was centrifuged for 4 min at 200g, then the fluid was decanted and the sediment was used for preparing smears on two microscope slides. After air drying, the smears were fixed with methyl alcohol and stained with azure eosin. The smears were microscoped with immersion at ×1000 magnification. The differential count for determining the percentage of AÌs, NLs, and other cells was conducted up to a total number of 100 counted cells. Allowing for the number of cells in the BALF, these percentages were recalculated in terms of absolute AM and NL counts.

### 2.2. The methodology of the system model's adjustment

#### 2.2.1. Estimates of the pulmonary deposition of inhaled NPs

For computing the $Fe_2O_3$-NP mass deposited from the inhaled air onto the free surface of the so-called pulmonary (or alveolar) region of the lower airways, we assumed that:

(a) The rat's minute respiratory ventilation was equal to 100 mL, which is 1.3 times higher than the lowest value found in the literature at 78 mL (Ramahandran, 2016) but 2.1 times lower as compared with the highest one at 210 mL (Maulderly and McCunney, 1997). In fact, this parameter as assessed experimentally by different authors varies broadly, but the published estimates do not exceed these limits.

(b) The pulmonary NP deposition fraction was equal to 0.52, which is close to the lowest of the differently substantiated assessments given by Kolanjiyil (2013). Taking into consideration that not only singlet but even compact aggregates of the inhaled NPs were in low nanoscale range we believe that this estimate is not too high.

Of course, both parameters are exact values but just estimates based on certain assumptions. However these assumptions do not go beyond the limit of the inevitable uncertainty permissible for system models of this kind.

#### 2.2.2. Identification of model's parameters for particle redistribution, elimination and retention

The starting point for our system modeling was the multicompartmental model of virtually insoluble particle distribution in, and elimination from the lungs based on imitation of the main physiological mechanisms presumably controlling these processes (Fig. 4).

This model had been developed earlier (Katsnelson et al., 1992) and proved adequate for simulating the pulmonary retention of inhaled mineral dusts (disintegration aerosols) particles characterized by different cytotoxicity degrees, including the most cytotoxic one, the DQ12 quartz (Katsnelson et al., 1997). For the latter, we had used the experimental data of Bellmann et al. (1991) rather than our findings as with all other dusts. Given the results obtained in the present long-term inhalation experiment with the $Fe_2O_3$, we decided to adjust this model to allow for them starting from the system of differential equations describing the pulmonary kinetics of just the DQ12 dust particles because of high cytotoxicity previously found for another nano-iron oxide, $Fe_3O_4$ (Katsnelson et al., 2010, 2011).

The so-called "identification" of a system model means finding the best numerical values of the differential equation system coefficients, which in our case play the part of kinetic constants, the ultimate goal being satisfactory quantitative simulation of the modeled process outcomes (in our case, pulmonary retention of inhaled particles in the course of a long-term exposure).

We had developed a methodology for this search when constructing previous multicompartmental models of the same kind. Essentially, this methodology presents an interplay between

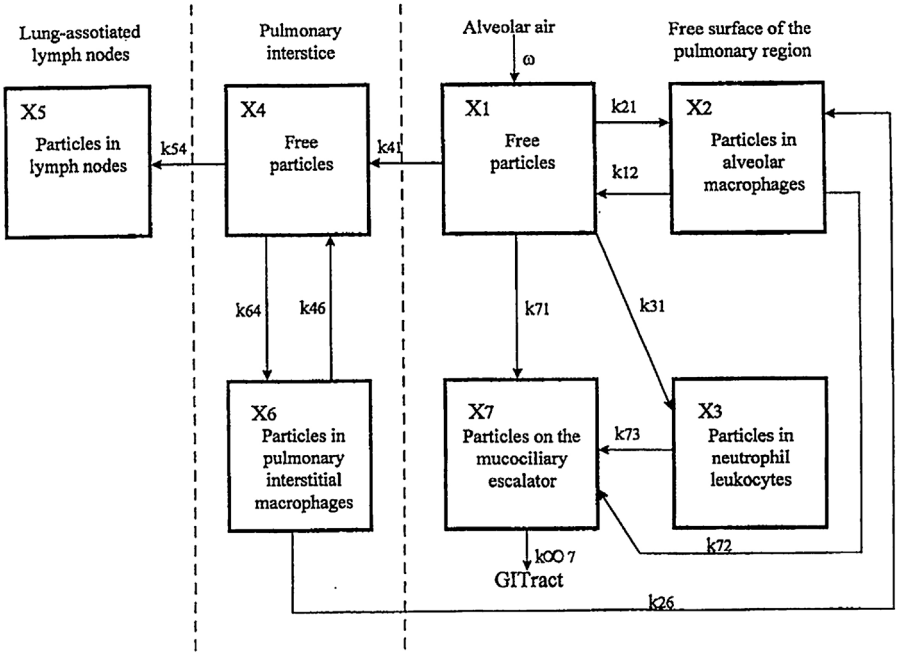


**Fig. 4.** Structure of the multicompartmental model for the kinetics of retention and clearance of insoluble dust particles deposited in the pulmonary region of the rat lung (Katsnelson et al., 1992, 1994, 1997) Dotted lines are conventional boundaries between anatomical regions.

a computerized programmed iteration procedure and some more or less important restrictions we impose on it regarding either the direction or the degree of change in certain constants, or both. These restrictions are usually based on either theoretical premises and/or experimental data, both our own and provided by other researchers, subject to the qualification, though, that neither ever give "exact values", just estimates, and therefore **a system model can give nothing but a more or less close approximation to reality**. Meanwhile, that is all that is often needed since system model identification is useful for proving the consistency of the model and thereby of the underlying *theory* rather than for predicting anything "reliably" for some practical use. Let us illustrate this approach with examples.

Thus, we thought it necessary to increase the $k_{41}$ constant of the particle transfer rate from compartment $X_1$ to compartment $X_4$, assuming that the ability of NPs to penetrate through the alveolar membrane towards the pulmonary interstice must be higher than that of the micrometric scale dust particles (quartzite rock, DQ12 quartz, $TiO_2$) used in the inhalation experiments based on which the original model was identified. However, having no data for deciding preliminarily how many fold increase in that constant would be justified mechanistically (and, moreover, considering that not only singlet NPs but also their aggregates do penetrate) we were unable to even hypothesize the extent of this change. So we could only set the direction of it. With this restriction, the said constant had to be adjusted by the iteration procedure, which resulted in its 4-fold increase.

The second example concerns our approach to modeling the toxicokinetic input of particle dissolution. In the above-described *in vitro* experiment it was found that $Fe_2O_3$-NPs collected from the exposure chamber exhaust provedvirtually insoluble in both de-ionized water and normal saline but dissolved slowly in model biological milieus: the cell-free broncho-alveolar lavage fluid (BALF) supernatant and in the sterile bovine blood serum (see Section 3.1).

Although we could have assumed that NPs dissolve *in vivo* wherever they are retained, we decided to allow for this process in the kinetics of retention of $Fe_2O_3$-NPs in the lungs by assuming it sufficient (and necessary, as we found it eventually) for the structure of the model to include elimination flows brought about by the dissolution of only free (i.e. extracellular) particles in compartment $X_1$ and $X_4$ (Fis. 4 and 5). When choosing the constant of rate $s_1$ for the first of these flows, it appeared quite justified to set as an orientation cue the value of 32 $weeks^{-1}$ found by us for the in vitro dissolution rate constant for $Fe_2O_3$-NPs from filter in the BALF supernatant, since this fluid is relatively similar to the milieu natural in which particles float on the free surface of the pulmonary region. The key word here is 'orientation' since the *in vivo* and *in vitro* constants cannot be equal in principle because: (a) BALF is diluted with the water used for lavage; (b) it is the finest NPs that reach the pulmonary region after inhalation (whereas the filter captured NPs from the chamber without preliminary separation by size); and (c) a proportion of the NPs that penetrated into the body of the filter were the least available for contact with the solvent.

It is even more difficult to identify a similar orientation cue for choosing the constant for the rate of elimination flow from compartment $X_4$ ($s_4$), primarily because for estimating this value *in vitro* it was difficult to find an adequate liquid medium that would be sufficiently close in composition and properties to the tissue fluid of the rat lungs. The sterile bovine blood serum used in this capacity seemed a comparatively suitable choice but, of course, it is far from being 'exact'. Moreover, the *in vitro* dissolution kinetics in this milieu was approximated by a two-exponential function on time. (see Section 3). We assumed that the finest NPs, which are most probably responsible for the quick dissolution phase, would have already dissolved before penetrating into the lung interstice. We therefore decided to make the elimination rate constant $s_4$ more or less close to the slow phase constant of the *in vitro* dissolution rate (4.9 $weeks^{-1}$). As a result, the iteration procedure oriented to the above estimates chose the values of the constants under consideration to be equal for $s_1 = 30\ weeks^{-1}$ and for $s_4 = 2.5\ weeks^{-1}$.

For describing the elimination of NPs from the lung-associated lymph nodes represented in the model by compartment $X_5$, we combined in one and the same quasi-flow the dissolution and the direct penetration of NPs into the lymph and blood, which can justify the higher value of the constant $s_5 = 6\ weeks^{-1}$ found by iteration.

As concerns the procedure of choosing the model's constants associated with particle phagocytosis, we propose, to make it easier to understand, to describe and exemplify it when discussing in the Section 4 some of the experimental findings that guided this choice.

## 3. Results

### 3.1. In vitro solubilization of $Fe_2O_3$-NPs

As is demonstrated by Fig. 6a, the iron oxide NPs collected from the air exhausted from the exposure chamber are virtually water-insoluble, and we might give here instead a quite analogous plot for a similar experiment with normal saline. However in both biological milieu tested these NPs were noticeably solubilized (Fig. 6b and c). The EPR signal decay in the BALF supernatant could be approximated by an exponential function with the dissolution rate coefficient $K = 32\ weeks^{-1}$ while that in the sterile bovine blood serum—by two exponential functions with $K_1 = 118\ weeks^{-1}$ and $K_2 = 4.9\ weeks^{-1}$.

**Table 1**
Cells in the broncho-alveolar lavage fluid of rats, x ± s.e.

| Rats exposed to: | Cell count $\times 10^6$ | | | |
|---|---|---|---|---|
| | Total | Alveolar macrophages (AMs) | Neutrophil leukocytes(NLs) | NL/AM count ratio |
| 24 h after the last exposure of the 3 month inhalation period[a] | | | | |
| $Fe_2O_3$-NPs inhalation | 2.45 ± 0.33* | 1.96 ± 0.28 | 0.46 ± 0.08* | 0.25 ± 0.02* |
| Sham (control) | 1.47 ± 0.23 | 1.35 ± 0.21 | 0.11 ± 0.03 | 0.08 ± 0.02 |
| 24 h after the intratracheal instillation (0.3 mg in 1 ml) | | | | |
| $Fe_2O_3$-NPs | 3.59 ± 0.24*+ | 2.69 ± 0.24 | 0.84 ± 0.09*+ | 0.35 ± 0.06* |
| Standard quartz DQ12 | 5.22 ± 0.32* | 3.09 ± 0.24* | 2.09 ± 0.41* | 0.85 ± 0.28* |
| Water (control) | 2.16 ± 0.26 | 2.04 ± 0.24 | 0.12 ± 0.03 | 0.05 ± 0.01 |

*Note*: *statistically significant ($p < 0.05$) difference from the control value; + the same from the value in the DQ12 group.
[a] Results for the 6- and 10-month inhalation periods are quite similar.

*Shifts in the BALF cellularity level and composition* induced by inhalation exposures to $Fe_2O_3$-NPs and by their intratracheal instillation (compared with that of the DQ12 quartz particles) are shown in Table 1.

### 3.2. Iron oxide nanoparticle retention

In the plot shown by Fig. 7 actual data on $Fe_2O_3$-NPs accumulation in lungs ($13.5 \pm 4.3$ μg for 3 month exposure, $11.5 \pm 6.5$ μg for 6 month exposure, $34.6 \pm 16.7$ μg for 10 month exposure) are superimposed on the curve in axes x (duration of experiment), y (mass of NPs in lungs) based on the model predictions. The TEM visualization of NPs in lungs and brain—by Figs. 8–10.

## 4. Discussion

When inhaled or instilled intratracheally, $Fe_2O_3$-NPs evoked a recruitment of alveolar macrophages (AMs) and, even more actively, of neutrophil leukocytes (NLs) onto the lower airways free surface with a significant increase in the NL/AM count ratio (Table 1, the upper 2 lines).

As is well known, neutrophil leukocyte (NL) recruitment towards the lower airways in response to the deposition of particles is traditionally described as "inflammation" and, thus, as a pathological phenomenon. This concept is common to nanotoxicological studies as well (e.g. Renwick et al., 2004; Stoeger et al., 2006; Sager et al., 2007; Grassian et al., 2007; Neuberger, 2007; Warheit et al., 2009; Liu et al., 2016). We always insist, however, that it can be misleading. Beyond any doubt, enhanced recruitment of NLs onto the free surface of the lower airways is typical of acute and, to a lesser degree, chronic inflammatory processes induced by microbial or chemical agents. However, a certain number of these cells is always present in the BALF of healthy animals, at least when they are constantly inhaling unfiltered air. Are they really living with chronic inflammation of their respiratory system?

Meanwhile, there are fairly strong reasons for considering the NL-associated response under discussion to be an important mechanism of compensation, even though incomplete, for the damage caused by cytotoxic particles to the AM, the undoubtedly main effecter of pulmonary clearance. We developed and identified a multicompartmental model of pulmonary region clearance which comprises this compensatory mechanism (Fig. 6) (Katsnelson et al., 1992, 1994, 1997). This model simulated very the well experimental data on the retention of virtually insoluble dust particles of various degrees of cytotoxicity (quartzite rock, titanium dioxide, standard quartz DQ12) in the lungs under long-term inhalation exposures and a decrease in this retention under the effect of glutamate, a potent protector of the macrophage against the cytotoxicity of particles (Morosova et al., 1982, 1984; Katsnelson et al., 1984a,b, 2014).

Note: ω is a function of particle deposition in the pulmonary region, and $\mathbf{k_{ji}}$ is a constant of the particles transfer rate from compartment $X_i$ into compartment $X_j$.

At the same time, persistent (non-dissolved) NPs are apparently more likely than microparticles to directly penetrate from the free surface of the alveoli not only into the pulmonary interstice and then on into the lymph, but also directly into the blood. Thus Zhu et al. (2009), who found $^{59}Fe$ in organs rich in mononuclear phagocytes as early as 10 min after intratracheal instillation of 22 nm $^{59}Fe_2O_3$ particles to rats, considered this to be evidence of direct passage of these particles through the alveolar-capillary barrier, the kinetics of which was described by the unicompartmental model.

It was long ago found and then repeatedly demonstrated in various experiments by our team that the NL recruitment is controlled by the mass of AM breakdown products and, thus, the more AMs are destroyed by the particles they have engulfed, the higher this recruitment (Privalova et al., 1980, 1987, 1995; Katsnelson and Privalova, 1984; Katsnelson et al., 1994, 1997, 1984a,b). That is why the NL/AM count ratio serves as a reliable, even if circumstantial, index of particle cytotoxicity. For instance, we demonstrated that, judging by this index, intratracheally instilled $Fe_3O_4$-NPs proved much more cytotoxic compared with 1 μm particles of this iron oxide. (Katsnelson et al., 2010, 2011).

.Meanwhile, as can be seen from the same Table 1 (the lower 3 lines), these cellular shifts in the BALF typical of immediate pulmonary responses to cytotoxic particle deposition were less pronounced for the $Fe_2O_3$-NPs compared with those evoked by the DQ12 particles. However, the AM recruitment induced by both particulates differed statistically insignificantly. Thus, the AM

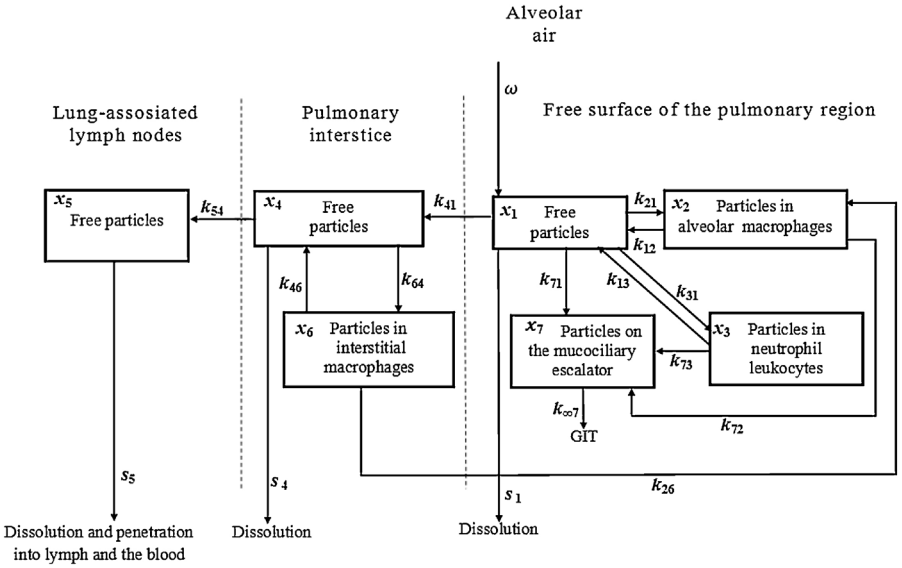


**Fig. 5.** Structure of the multi-compartmental model for the kinetics of retention and elimination of the $Fe_2O_3$-NPs deposited in the pulmonary region of the lung. Here: $\omega$ is a function of particle deposition in the pulmonary region, and $k_{ji}$ is a rate constant of particle translocation from compartment Xi into compartment Xj. Dotted lines are conventional boundaries between anatomical regions.

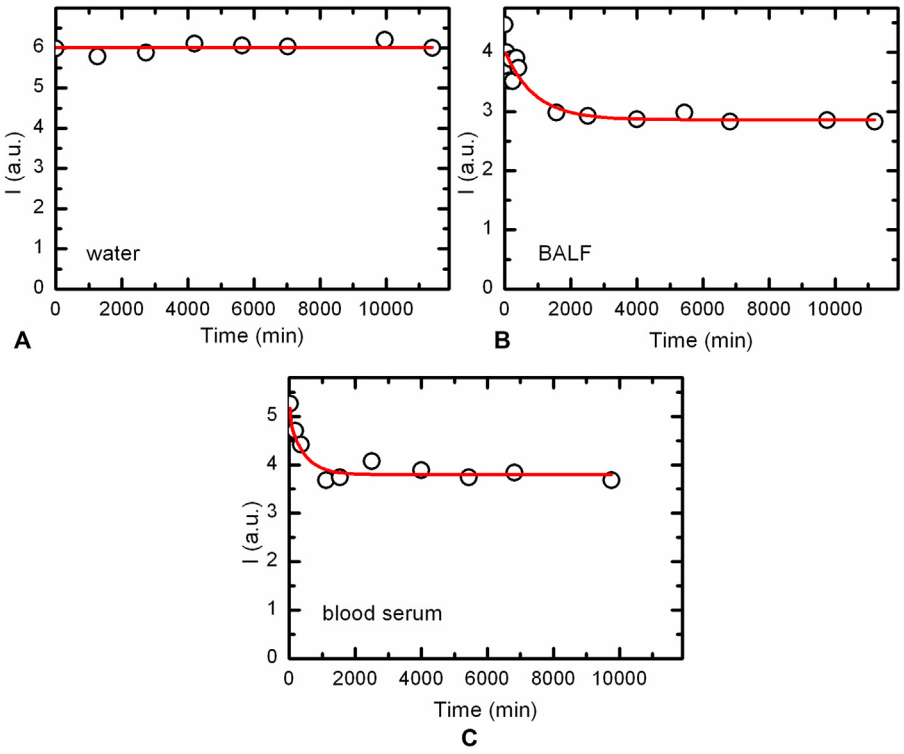


**Fig. 6.** The kinetics of the decay of the $Fe_2O_3$ EPR signal intensity (I) in arbitrary units (a.u.) from NPs collected on the PSI filter and incubated in: (A) water or normal saline; (B) the BALF supernatant; (C) the sterile bovine blood serum.

response may be regarded as almost equally engaged in the elimination of particles of both types, and we assumed that even a statistically significant difference in the involvement of the compensatory NL phagocytosis could fail to play a substantial toxicokinetic role.

In other words, we did not have reliably experimentally supported quantitative restrictions for the iteration program to choose model constants associated with particle phagocytosis. However, there were certain justified **limitations and orientation cues** of this choice. Thus, based on the higher phagocytic activity of AMs compared with NLs in relation to any particles, including iron oxide NPs (Katsnelson et al., 2010, 2011), we set the condition $k_{21} > k_{31.}$ Given the fact that the rate of secondary release of phagocytized particles as a result of breakdown of the cell pool is naturally lower than the rate of engulfment, we could have set the conditions $k_{21} > k_{12,}$ $k_{31} > k_{13}$ and $k_{64} > k_{46}$. Since the relatively low burden of a unit NL with particles renders the probability of its damage by these particles and the consequent breakdown low compared with that for a unit AM, we assumed the condition $k_{13} << k_{12}$ (As can be seen from Fig. 1, this breakdown was not taken into account by the original model as being negligibly small).

At the same time, we are unaware of any data on the comparative phagocytic activity of AMs and interstitial pulmonary macrophages, while the ratio between the numbers of available pools of these cells is known to be dynamic, which in aggregate makes it impossible to set the condition of this or that inequality of the constants $k_{21}$ and $k_{64.}$ We could only suppose that they are really unequal rather than identical. On the other hand, both the original (Fig. 1) and the present (Fig. 5) system model assumed that, whatever variant of cell death (apoptosis, autophagy or necrosis) is predominantly involved in the discussed damage to the particle-loaded macrophage or the NL and then in their breakdown, the immediate toxicokinetic outcome of this breakdown within the framework of the system model is essentially the same: de-internalization of the previously internalized particles. Even if this assumption somewhat simplifies the reality, we should stress once again that such a simplification is both inevitable and permissible for any model of system.

However, even a virtually unrestricted iteration procedure dealing with only these cell-dependent constants plus increasing the constant $k_{41}$ as proposed in Section 2.2.2 proved incapable of simulating satisfactorily our actual data on pulmonary $Fe_2O_3$-NPs retention. Thus the next well justified step was to include into the model additional elimination flows described in that Section and to re-identify the whole model thus modified.

As can be seen from Fig. 7, the model thus adjusted predicted the time course of the increase in the $Fe_2O_3$ pulmonary burden as a curve, gradually reaching a plateau, which is typical of the 1st order toxicokinetics. At each time point of our experiment this curve is situated within 95% CI of the mean factual mass of $Fe_2O_3$—NPs found in rat lungs. In other words, the deviation of the experimental data from this prediction is **not statistically significant**, and thus they corroborate fairly well the model's imitation of the NP retention process and, thereby, its mechanistic premises.[1]

[1] It may be worthwhile to remind that we are dealing with a **system model** (specifically, the so-called architectural modeling which uses the systems architecture to conceptually model the structure and behavior of a system) instead of a **data model**, which, in this case. would approximate the actual experimental data by a simply linear relationship with time of exposure. These two major classes of mathematical models differ not only in their philosophy and intended purpose but also in the mode of using actual (in particular, experimentally obtained) values. While in the data modelling parameters of a mathematical expression and its graphical interpretation are being directly fitted to these values (e.g. with the least squares technique), in the system modelling they are being compared iteratively with those inferred from theoretically justified mathematical expression(s) imitating a real system. Due both to inevitable simplification of the latter by the former and to the usual sampling errors in experimental results, these results and model predictions often do not exactly match together. However if difference between them is not significant statistically, a prediction can be considered as coming true.

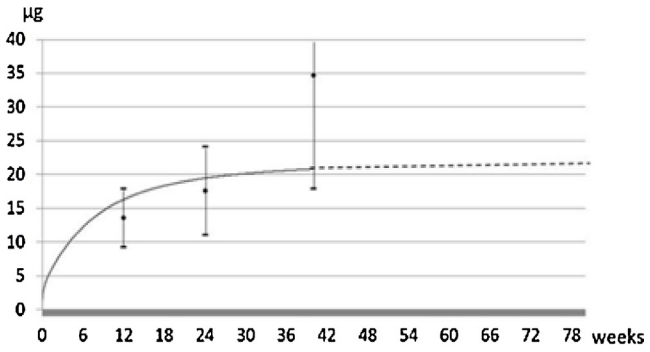


**Fig. 7.** Kinetics of $Fe_2O_3$-NPs accumulation in the lungs of rats as predicted by the adjusted multi-compartmental model (see Fig. 5) for the actual exposure period (the solid line) and later on (dashed line). Dots with bars are experimental results with 95% CI. The abscissas represent weeks from the start of the exposures; and the ordinates, the $Fe_2O_3$ content of the lungs, mcg.

In particular, it should be stressed that these results agree with the important toxicokinetic role played by the *in vivo* solubilization of the metal oxide NPs which process imitation was necessary to be included into the model whose predictions proved otherwise to be far off the mark. Let us say in parentheses that just this process probably explains why the actual retention of $Fe_2O_3$ in the lungs of the rats in our experiment was many times lower than the retention of $SiO_2$ in the quite similar conditions of the experiment with DQ12 (Bellmann et al., 1991). Thus, at 3 and 9 month time points it was 207 μg and 550 μg, respectively (cf. 13.5 μg and 34.6 μg Fe2O3 at 3 and 10 month time points of our experiment).

As for the accumulation of $Fe_2O_3$-NPs in the lung-associated lymph nodes, unfortunately we have just one experimental result obtained for a pooled tissue sample in the group in relation to the 10-month time-point; and this result (0.003 μg) is close enough to the model prediction (0.004 μg). Again, this accumulation is far lower than that of $SiO_2$ in the experiment with DQ12 (103 μg).

Figs. 8 and 9 illustrate the TEM-visualization of the NPs accumulated within the alveolocytes of both Type I and Type II. From the toxicokinetic point of view, this accumulation may be assumed to be an intermediary phase of free NP transfer across the alveolar membrane (i.e. from compartment $X_1$ towards compartment $X_4$). This transfer is described by our model as a passive diffusion process whereas in reality it may have an active physiological (cell-mediated) component as well. On the other hand, we see that alveolocytes can be damaged while taking part in this transfer of cytotoxic NPs.

We also saw NPs in the olfactory region of the brain (Fig. 10), where they were detected only within the myelin sheaths of the intracerebral nervous fibers (with focal demyelinization). Such bizarre localization seems to testify to NP translocation from the nasal cavity along the olfactory nerve fibers as the most probable pathway. As is well known, this pathway has been directly proven by many experiments (e.g. Oberdörster et al., 2004; Elder et al., 2006; Kao et al., 2012). However, the total brain accumulation of $Fe_2O_3$ was too low to be detected by the EPR, which made it impossible for us to identify a model that would simulate the nasal deposition and nose-to-brain translocation of NPs.

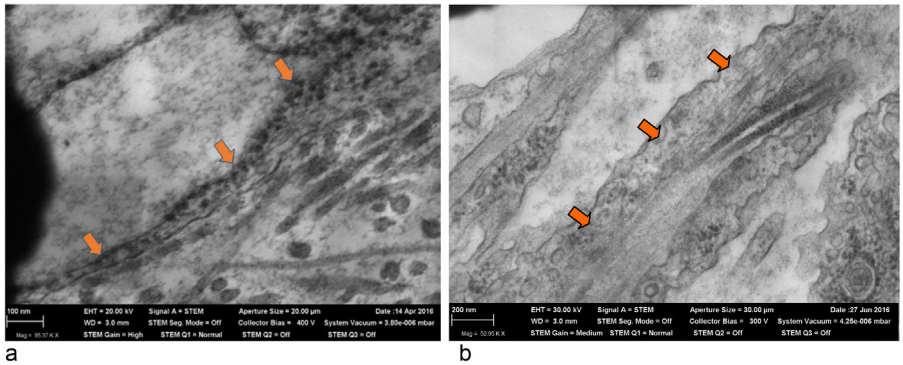


**Fig. 8.** Type I alveolocytes (pointed by arrows) in the lung of: (a) a rat after 6-month inhalation exposure, with a lot of internalized NPs (TEM, magnification × 95,370); (b) a sham-exposed rat without discernible NPs (TEM, magnification × 52950).

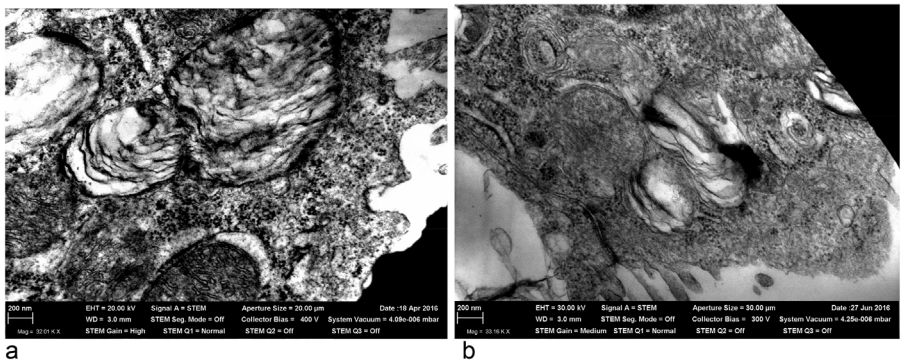


**Fig. 9.** The type II alveolocytes in the lung of (a) a rat after 6-month inhalation exposure with a lot of internalized NPs (TEM, magnification × 32,010); a sham-exposed rat with a far less number of them (TEM, magnification × 33,160).

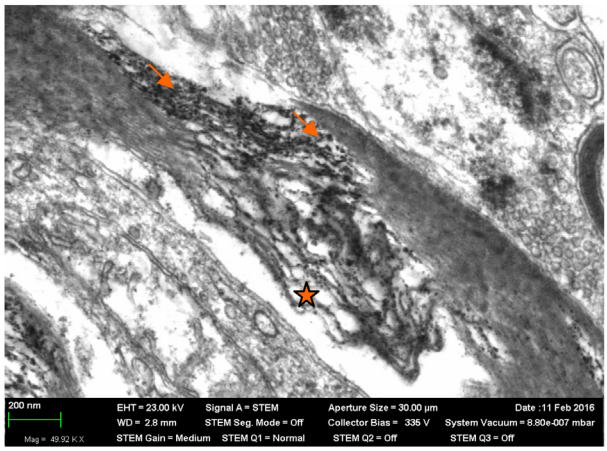


**Fig. 10.** A longitudinal section of a nerve fiber in the olfactory brain region of a rat after 10-month inhalation exposure. Note focal damage to the myelin sheath (marked by an asterisk) associated with accumulation of the NPs pointed by arrows (TEM, magnification × 49,920).

## 5. Conclusion

The metal oxide NP long-term pulmonary toxicokinetics is most probably controlled by both physiological and physico-chemical mechanisms, namely their ability to penetrate through membranes or to be internalized by macrophages, neutrophils and alveolocytes, and their *in vivo* dissolution. It may be hypothesized that the relative contribution of this or that mechanism depends on the size and chemical nature of nanoparticles under consideration. It should be stressed that neither scarce and rather contradictory data of the relevant literature, nor our study in which we dealt with NPs of only one chemical composition having dimensions within a rather narrow low nanometric range, are sufficient for regarding this hypothesis as a well proven general theory. However, with this qualification, we maintain that in the specific case of 14 nm $Fe_2O_3$ particles, our experimental data in a satisfactory agreement with the predictions of the adjusted mechanistic multicompartmental model, demonstrated the most important toxicokinetic role of these NP solubilization in the biological milieu with a less important but still noticeable input of phagocytosis-dependent pulmonary clearance mechanisms

The deposition and retention of metal oxide NPs in the lungs, even if rather low and even if the metal is of a relatively low toxicity, is associated with some cytotoxic effects. Our model takes into account the toxicokinetic consequences of cytotoxic damage to the alveolar macrophage with compensatory recruitment of neutrophil leukocytes. Eventually, we should also try and incorporate into this model the possible toxicokinetic repercussions of the NP-induced damage to alveolocytes.

## Conflict of interest

None.

## References


Adamcakova-Dodd, A., Stebounova, L.V., Kim, J.S., Vorrink, S.U., Ault, A.P., O'shaughnessy, P.T., Grassian, V.H., Thorne, P.S., 2014. Toxicity assessment of zinc oxide nanoparticles using sub-acute and sub-chronic murine inhalation models. Part. Fibre Toxicol. 11, 15.

Bellmann, B., Creutzenberg, O., Dasenbrock, C., 1991. Lung clearance and retention of toner utilizing a tracer technique, during chronic inhalation exposure in rats. Fundam. Appl. Toxicol. 17, 300–313.

Creutzenberg, O., 2013. Toxic Effects of Various Modifications of a Nanoparticle Following Inhalation (Research Project F 2246). The Federal Institute for Occupational Safety and Health, Dortmund, Berlin, Dresden p. 405.

Dumkova, J., Vrlikova, L., Vecera, Z., Putnova, B., Docekal, B., Mikuska, P., Fictum, P., Hampl, A., Buchtova, V., 2016. Inhaled cadmium oxide nanoparticles: their in vivo fate and effect on target organs. Int. J. Mol. Sci. 17 (6), 874.

Elder, A., Gelein, R., Silva, V., Feikert, T., Opanashuk, L., Carter, J., Potter, R., Maynard, A., Ito, Y., Finkelstein, J., Oberdörster, G., 2006. Translocation of inhaled ultrafine manganese oxide particles to the central nervous system. Environ. Health Perspect. 114 (8), 1172–1178.

Ennan, A.A., Kiro, S.A., Oprya, M.V., Vishnyakov, V.I., 2013. Particle size distribution of welding fume and its dependency on conditions of shielded metal arc welding. J. Aerosol Sci. 65, 103–110.

Grassian, V.H., O'Shaughnessy, P.T., Adamcakova-Dodd, A., Pettibone, J.M., Thorne, P. S., 2007. Inhalation exposure study of titanium dioxide nanoparticles with a primary particle size of 2 to 5 nm. Environ. Health Perspect. 115, 397–402.

ICRP, 1994. Publication 66: human respiratory tract model for radiological protection. A Report of a Task Group of the International Commission on Radiological Protection, 24. Ann. ICRP, pp. 1–482.

International Institute of Welding, 2009. International Seminar Exposure to Ultrafine Particles in Welding Fumes, Hannover.

Kao, Y.-Y., Cheng, T.-J., Yang, D.-M., Liu, P.-Sh., 2012. Demonstration of an olfactory bulb–brain translocation pathway for ZnO nanoparticles in rodent ells in vitro and in vivo. J. Mol. Neurosci. 48 (2), 464–471.

Katsnelson, B.A., Privalova, L.I., 1984. Recruitment of phagocytizing cells into the respiratory tract as a response to the cytotoxic action of deposited particles. Environ. Health Perspect. 55, 313–325.

Katsnelson, B.A., Morosova, K.I., Velichkovski, B.T., et al., 1984a. Antisilikotische Wirkung von Glutamat. Arbeitsmed. Sozialmed. Präventivmed. 19 (7), 153–156.

Katsnelson, B.A., Privalova, L.I., Kislitsina, N.S., Podgaiko, G.A., 1984b. Correlation between cytotoxicity and fibrogenicity of silicosis-inducing dusts. Med. Lav. 75, 450–462.

Katsnelson, B.A., Konysheva, L.K., Privalova, L.I., Morosova, K.I., 1992. Development of a multicompartmental model of the kinetics of quartz dust in the pulmonary region of the lung during chronic inhalation exposure of rats. Br. J. Ind. Med. 49, 172–181.

Katsnelson, B.A., Konyscheva, L.K., Sharapova, N.Ye., Privalova, L.I., 1994. Prediction of the comparative intensity of pneumoconiotic changes caused by chronic inhalation exposure to dusts of different cytotoxicity by means of a mathematical model. Occup. Environ. Med. 51, 173–180.

Katsnelson, B.A., Konysheva, L.K., Privalova, L.Y., Sharapova, N.Y., 1997. Quartz dust retention in rat lungs under chronic exposure simulated by a multicompartmental model: further evidence of the key role of the cytotoxicity of quartz particles. Inhal. Toxicol. 9, 703–715.

Katsnelson, B.A., Privalova, L.I., Kuzmin, S.V., Degtyareva, T.D., Sutunkova, M.P., Yeremenko, O.S., 2010. Some peculiarities of pulmonary clearance mechanisms in rats after intratracheal instillation of magnetite ($Fe_3O_4$) suspensions with different particle sizes in the nanometer and micrometer ranges: are we defenseless against nanoparticles? Int. J. Occup. Environ. Health 16, 508–524.

Katsnelson, B.A., Privalova, L.I., Degtyareva, T.D., Sutunkova, M.P., Yeremenko, O.S., Minigalieva, I.A., 2011. Experimental estimates of the toxicity of iron oxide $Fe_3O_4$ (magnetite) nanoparticles. Cent. Eur. J. Occup. Environ. Med. 16, 47–63.

Katsnelson, B.A., Privalova, L.I., Kuzmin, S.V., Gurvich, V.B., Sutunkova, M.P., Kireyeva, E.P., Minigalieva, I.A., 2012. An approach to tentative reference levels setting for nanoparticles in the workroom air based on comparing their toxicity with that of their micrometric counterparts—a case study of iron oxide $Fe_3O_4$. ISRN Nanotechnol. 2012 (2012) Article ID 143613, 12 pages.

Katsnelson, B.A., Privalova, L.I., Gurvich, V.B., Makeyev, O.H., Shur, V.Y., Beikin, J.B., 2013. Comparative in vivo assessment of some adverse bio-effects of equidimensional gold and silver nanoparticles and the attenuation of nanosilver's effects with a complex of innocuous bioprotectors. Int. J. Mol. Sci. 14, 2449–2483.

Katsnelson, B.A., Privalova, L.I., Gurvich, V.B., Kuzmin V, S., Kireyeva, E.P., Minigalieva, I.A., Sutunkova et al, M.P., 2014. Enhancing population's resistance to toxic exposures as an auxilliary tool of decreasing environmental and occupational health risks (a self-overview). J. Environ. Prot. 5, 1435–1449 Special Issue Environment Contamination and Toxicology.

Katsnelson, B.A., Privalova, L.I., Sutunkova, M.P., Gurvich, V.B., Loginova, N.V., Minigalieva, I.A., et al., 2015. Some inferences from in vivoexperiments with metal and metal oxide nanoparticles: the pulmonary phagocytosis response, subchronic systemic toxicity and genotoxicity, regulatory proposals, searching for bioprotectors (a self-overview). Int. J. Nanomed. 10, 3013–3029.

Kolanjiyil, A.V., 2013. Deposited nanomaterial mass transfer from lung airways to systemic regions. A Thesis for MSc Degree. North Cariolina State University, Raleigh, NC.

Kreyling, W.G., Semmler-Behnke, M., Takenaka, S., Möller, W., 2013. Differences in the biokinetics of inhaled nano- versus micron-sized particles. Acc. Chem. Res. 46 (3), 714–722.

Lehnert, M., Pesch, B., Lotz, A., Pelzer, J., Kendzia, B., Gawrych, K., Heinze, E., Van Gelder, R., Punkenburg, E., Weiss, T., Mattenklott, M., Hahn, J.U., Möhlmann, C., Berges, M., Hartwig, A., Brüning, T., 2012. Exposure to inhalable, respirable, and ultrafine particles in welding fume. Ann. Occup. Hyg. 56 (5), 557–567.

Lewinski, N., Graczyk, H., Riediker, M., 2013. Human inhalation exposure to iron oxide particles. BioNanoMat 14 (1–2), 5–23.

Liu, J., Feng, X., Wei, L., Chen, L., Song, B., Shao, L., 2016. The toxicology of ion-shedding zinc oxide nanoparticles. Crit. Rev. Toxicol. 46 (4), 348–384.

Maulderly, J.L., McCunney, R.G., 1997. Particle overload in the rat lung and lung cancer. Implications for Human Risk Assessment. Taylor & Francis, Philadelphia, USA.

Minigalieva, I.A., Katsnelson, B.A., Privalova, L.I., Sutunkova, M.P., Gurvich, V.B., Shur, V.Y., et al., 2015. Attenuation of combined nickel (II) oxide and manganese (II, III) oxide nanoparticles' adverse effects with a complex of bioprotectors. Int. J. Mol. Sci. 16 (9), 22555–22583.

Morosova, K.I., Aronova, G.V., Katsnelson, B.A., 1982. On the defensive action of glutamate on the cytotoxicity and fibrogenicity of quartz dust. Br. J. Ind. Med. 39 (3), 244–252.

Morosova, K.I., Katsnelson, B.A., Rotenberg, Yu.S., Belobragina, G.V., 1984. A further experimental study of antisilicotic effect of glutamate. Br. J. Ind. Med. 41 (4), 518–525.

Neuberger, M., 2007. Umweltepidemiologie und Toxikologie von Nanopartikeln. In: Gazsó, A., Greßler, S., Schiemer, F. (Eds.), Nano–Chancen und Risiken aktueller Technologien. Springer, Wien, New York, pp. 181–197.

Oberdörster, G., Sharp, Z., Atudore, V., Elder, A., Gelein, R., Kreylin, W., 2004. Translocation of inhaled ultrafine particle to the brainI. Inhal. Toxicol. 16 (6/7), 437–445.

Petin, L.M., 1978. Data for establishing the maximal allowable concentration of silica-containing condensation aerosols. Gigiyena Truda 6, 28–33 Russian.

Podgayko, G.A., Katsnelson, B.A., Lemyasev, M.F., Solomina, S.N., Saitov, V.A., Russjayeva, L.V., 1982. New data for assessment of the silicosis risks due to industrial aerosols based on a colloidal solution of silicic acid. In: Domnin, S.G., Katsnelson, B.A. (Eds.), Occupational Diseases Due to Dusts. Erisman's Institute, Moscow (Issue 7).

Privalova, L.I., Katsnelson, B.A., Osipenko, A.B., Yushkov, B.H., Babushkina, L.G., 1980. Response of a phagocyte cell system to products of macrophage breakdown as a probable mechanism of alveolar phagocytosis adaptation to deposition of particles of different cytotoxicity. Environ. Health Perspect. 35, 205–218.

Privalova, L.I., Katsnelson, B.A., Yelnichnykh, L.N., 1987. Some peculiarities of the pulmonary phagocytotic response, dust kinetics, and silicosis development during long term exposure of rats to high quartz levels. Br. J. Ind. Med. 44, 228–235.

Privalova, L.I., Katsnelson, B.A., Sharapova, N.Y., Kislitsina, N.S., 1995. On the relationship between activation and the breakdown of macrophages in pathogenesis of silicosis. Med. Lav. 86, 511–521.

Privalova, L.I., Katsnelson, B.A., Loginova, N.V., Gurvich, V.B., Shur, V.Y., Valamina, I. E., 2014. Subchronic toxicity of copper oxide nanoparticles and its attenuation with the help of a combination of bioprotectors. Int. J. Mol. Sci. 15, 12379–12406.

Ramahandran, G., 2016. Assessing Nanoparticle Risk to Human Health. Elsevier, Amsterdam.

Renwick, L., Brown, D., Clouter, K., Donaldson, K., 2004. Increased inflammation and altered macrophage chemotactic responses caused by two ultrafine particle types. Occup. Environ. Med. 61, 442–447.

Sager, T.M., Porter, D.W., Robinson, V.A., Lindsley, W.G., Schwegler-Berry, V.A., Castranova, V., 2007. Improved method to disperse nanoparticles in vitro and in vivo investigation of toxicity. Nanotoxicology 1, 118–129.

Stoeger, T., Reinhard, C., Takenaka, Sh., Schroeppel, A., Karg, E., Ritter, B., 2006. Instillation of six different ultrafine carbon particles indicates a surface area threshold dose for acute lung inflammation in mice. Environ. Health Perspect. 114 (3), 328–333.

Utembe, W., Potgieter, K., Stefaniak, A.B., Gulumian, M., 2015. Dissolution and biodurability: important parameters needed for risk assessment of nanomaterials. Part. Fibre Toxicol. 12 (11) .

Warheit, D.B., Reed, K.L., Sayes, C.M., 2009. A role fore surface reactivity in $TiO_2$ and quartz-related nanoparticle pulmonary toxicity. Nanotoxicology 3, 181–187.

Zhu, M.T., Feng, W.Y., Wang, Y., Wang, B., Wang, M., Ouyang, H., 2009. Particokinetics and extrapulmonary translocation of intratracheally instilled ferric oxide nanoparticles in rats and the potential health risk assessment. Toxicol. Sci. 107 (2), 342–351.